*Int. J. Electrochem. Sci.*, 16 **(2021)** Article Number: 21127, doi: 10.20964/2021.12.13

International Journal of
ELECTROCHEMICAL
SCIENCE
www.electrochemsci.org

# Electrochemical Behavior of n-tricalcium Phosphate and Graphene Oxide/Chitosan /n-tricalcium Phosphate Composite Coated Ti Metal, Ti-6Al-4V, and Co-Cr-W Alloys in Artificial Serum

*Reham H. Tammam*[1,*], *A. S. Mogoda*[1], *H. H. Abo-almaged*[2], *Sara G. Abd El-Kader*[1]

[1] Chemistry Department, Faculty of Science, Cairo University, Giza 12613, Egypt
[2] Refractories, Ceramic and Building Materials Department, Inorganic Chemical Industries and Mineral Resources Division, National Research Centre (NRC), Cairo, 12622, Egypt
[*]E-mail: reham_tammam@cu.edu.eg

*Received:* 11 June 2021 / *Accepted:* 2 August 2021 / *Published:* 10 November 2021

Nano-tricalcium phosphate (n-TCP) was prepared and its characterization was examined by X-ray diffraction, Transmission electron microscopy, and Scanning electron microscopy (SEM). The effects of coating of Ti metal, Ti-6Al-4V (TAV), and Co-Cr-W alloys with n-TCP or with graphene oxide/chitosan/n-tricalcium phosphate (GO/CS/n-TCP) composite on their corrosion in artificial serum were investigated by open circuit potential(OCP) and electrochemical impedance spectroscopy (EIS) techniques. The OCP of the uncoated, n-TCP coated, and GO/CS/n-TCP composite coated titanium metal, TAV, and Co-Cr-W alloys increase to a more positive value with time for about one hour before reaching a steady-state value in serum due to the growth of the air formed film on the surfaces of the materials. A two-time constants equivalent electrical circuit was used for fitting the experimental EIS results which were suitable for the passive film on the examined materials that consists of a barrier inner layer and a porous outer one. The impedance results revealed that the corrosion resistance increases with time and then decreases after 21 days as a result of the partial decomposition of the protective film on the surface of the electrodes. For all the studied materials here the corrosion resistance of their surfaces follows the order uncoated <n-TCP coated < GO/CS/n-TCP composite coated. Hence, coating of the tested material surface with n-TCP or composite assists the process of the passive film growth with time till a definite thickness but for a long time, this protective layer dissolves to a certain limit. SEM micrograph of the graphene oxide/chitosan/n-tricalcium phosphate composite coated Co-Cr-W alloy revealed that the composite contains very small pores which help the diffusion of ions through it causing the growth of the protective film on the alloy surface with time.

**Keywords:** Titanium; TAV; Co-Cr-W; n-TCP;EIS; SEM

## 1. INTRODUCTION

Titanium and its alloys, in addition to cobalt chromium-based alloys, had been used as biomedical implants due to their excessive corrosion resistance and top mechanical residences but they're now not sufficiently bioactive and consequently, surface change is necessary to enhance the bioactivity and osseointegration with bone tissues. This can be done using a bioactive coating such as calcium phosphate which is a truly bone-bonding material [1-4]. Techniques such as electrochemical deposition, plasma-spraying, and vapor deposition produce dense coatings making the implant surface homogeneously. The electrochemical deposition optimizes the technical parameters that lead to the extraordinary structure and characteristics of the coating substance. Electrochemical deposition of nano-tetra calcium phosphate on titanium led to considerable corrosion safety within the body fluid solutions when in comparison with uncoated titanium metal [5].

CS has wonderful biocompatibility, biodegradability, antibacterial properties [6, 7] and can activate the differentiation of osteoprogenitor cells, and therefore, facilitate bone repair and regeneration [8]. GO has many feature properties which include high specific surface area, excellent mechanical properties, properly dispensability in both water and some organic solvents, acceptable biocompatibility, and antibacterial properties, consequently it is normally utilized as a gene or drug delivery system, biosensor, hydrogel, and tissue engineering [9-15]. GO/CS films containing antibiotics has been prepared through electrophoretic deposition (EPD), and the films confirmed high bactericidal assets [16]. Calcium carbonate/ multiwalled-carbon nanotubes/ chitosan composite coating on TAV alloy was fabricated by electroless deposition and enhanced the corrosion resistance of the alloy [17].

The potentiodynamic polarization of Graphene oxide–chitosan–hydroxyapatite composite coated Ti in artificial body fluid revealed that this coating which is fabricated by EPD protects Ti substrate from corrosion [18]. The potentiostat deposition of polypyrrole/chitosan composite coating on titanium enhanced hardness and adhesion strength compared to the polypyrrole coating. Also, the polypyrrole/chitosan composite coating improved the corrosion resistance and biocompatibility of the Ti implant [19]. Electrophoretic deposition of the bioactive hydroxyapatite/graphene composite on Ti in simulated body fluid solutions resulted in the formation of apatite layer which enhanced the corrosion stability of the metal[20].

However, the research on the electrochemical behavior of Ti, TAV, and Co-Cr-W alloys protected through bioactive coatings in the artificial serum is very uncommon. The present work interests with the stability of Ti, TAV, and Co-Cr-W alloys in the artificial serum solution. Also, we investigate the corrosion behavior of n-TCP and GO/CS/n-TCP composite coated Ti metal, TAV, and Co-Cr-W alloys in the test solution. The study was carried out using OCP and EIS techniques. The surface morphology of the graphene oxide/chitosan/n-tricalcium phosphate composite coated Co-Cr-W alloy was identified by SEM.

## 2. EXPERIMENTAL

### *2.1. Electrodes*

Titanium (99.99%), TAV, and Co-Cr-W alloys of the compositions given in Table 1 had been fixed into glass tubes with epoxy resin leaving surface areas of 0.315, 0.503, and 0.594 $cm^2$ for titanium, TAV alloy and Co-Cr-W alloy, respectively.

**Table 1.** Compositions of the studied materials.

| **TAV** | Ti | Al | V | Fe | O | C | N | |
|---|---|---|---|---|---|---|---|---|
| (wt. %) | 90.091 | 5.70 | 3.85 | 0.180 | 0.106 | 0.038 | 0.035 | |
| **Co-Cr-W** | Co | Cr | W | Mo | Nb | Fe | Mn | Si |
| (wt. %) | 61 | 24 | 8 | 2.5 | 1 | 1 | 1 | 1 |

### *2.2. Specimen and solution preparation.*

The working electrodes had been polished before immersion in the electrolyte using successively grades emery papers from six hundred to two thousand grit, then rubbed with a smooth cloth until they became like a mirror surface and washed with doubly distilled water. The composition of the artificial serum of pH 7.0 is shown in Table 2 [21].

**Table 2.** The composition of the artificial serum of pH 7.0.

| **Compound** | **Concentration (mM)** | **Compound** | **Concentration (mM)** |
|---|---|---|---|
| **D,L-alanine** | 0.41 | D,L-methionine | 0.034 |
| **L-arginine** | 0.21 | L-phenylalanine | 0.16 |
| **L-aspartic acid** | 0.88 | L-serine | 0.16 |
| **L-cysteine** | 0.07 | D,L-tryptophan | 0.085 |
| **glycine** | 0.14 | NaHCO3 | 8.0 |
| **L-histidine** | 0.14 | NaCl | 88.8 |
| **L-lysine** | 0.20 | Citric acid | 0.17 |

### *2.3. Synthesis of n-TCP*

Nano-sized calcium phosphate particles were prepared by the sol-gel method via the slow addition of potassium dihydrogen phosphate solution (0.67 M) to calcium nitrate solution (1.0 M) under continuous stirring [22]. Tricalcium phosphate was precipitated as a white precipitate through the addition of ammonia solution dropwise to the above mixture to adjuste the pH at 10. The precipitate was stirred for 1 hour and aged at room temperature for 48 hours then filtrated and washed

with warm distilled water. The obtained powder was dried at 40°C overnight and undergone thermal treatment at 800°C for one hour with a heating rate of 10 °C/min.

### *2.4. Analysis methods of n-TCP*

The crystalline phases of n-TCP powder were analysed by X-ray diffraction (Bruker D8 Advance-Germany using a Ni filter, Copper Target, at V=40 kV and A=40 mA). The morphology and particle size of the n-TCP powder were investigated by transmission electron microscopy (JEOL JEM-1230, Tokyo, Japan). The microstructures of n-TCP powder and GO/CS/n-TCP composite coated Co-Cr-W alloy were examined by SEM (Philips XL30).

### *2.5. Deposition of n-TCP and GO/CS/n-TCP composite coatings*

Before coating with n-TCP, the sample surface was abraded and used as cathode and platinum counter electrode was used as anode. The coating was carried out using a slightly supersaturated solution of n-TCP at neutral pH at a constant potential of – 1.7 V 30 min. The pH was adjusted using Na $HCO_3$ solution.

Sample coating with GO/CS/n-TCP composite was carried out in a bath which consists of: 1-0.50 g of CS in 98 ml water and 2 ml of glacial acetic acid, 2- GO was dispersed by ultrasonic in 80 vol % ethanol overnight and stirred for 4 h with a concentration of 0.044 mg/ml, 3- slightly supersaturated solution of n-TCP. The coating process was carried at – 1.7 V for 30 min.

### *2.6. Electrochemical measurements*

The OCP and impedance were measured via the electrochemical workstation IM6 Zahner elektrik (Meβtechnik, Germany) [23]. The amplitude of input signal was 10 mV peak to peak in the frequency range 0.1 – $10^5$ Hz. The electrolytic cell was a three-electrode glass cell. A Pt sheet was used as an auxiliary electrode and the OCP was measured versus a saturated calomel electrode as a reference electrode.

## 3. RESULTS AND DISCUSSION

### *3.1. Characterization of nano-tricalcium phosphate*

Figure 1 shows the X-ray diffraction pattern of the prepared n-TCP powder. The results confirm the presence of all major TCP peaks matching the ICDD standard for tricalcium phosphate (JCPDS card no. 76-2065).

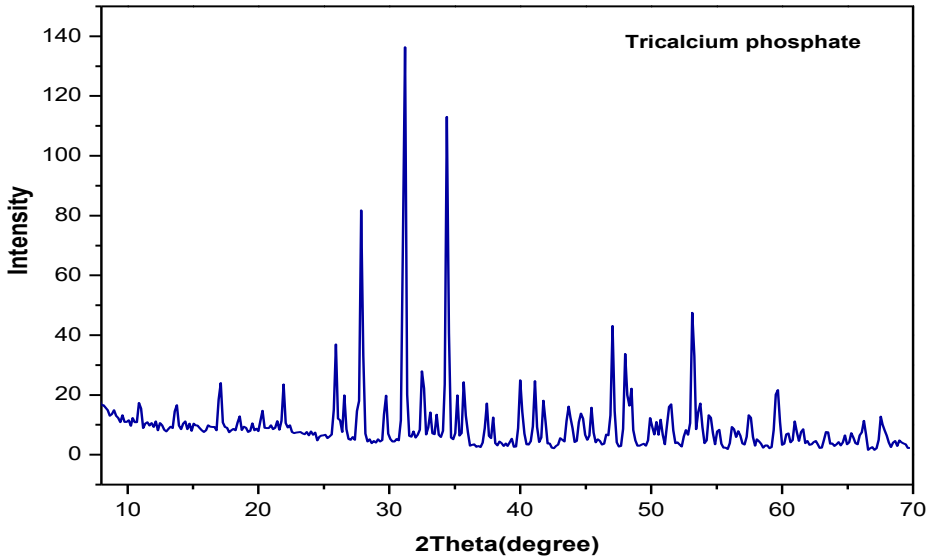


**Figure 1.** XRD pattern of the prepared n-TCP powder.

The TEM micrographs of the prepared n-TCP are shown in Figure 2a and b at two different magnifications. The average particle size of n-TCP grains lies in the nano range between 4.3 to 10.14 nm. The grains appeared in a prismatic shape with an agglomeration of nano β-TCP due to the large surface area associated with these nanoparticles.

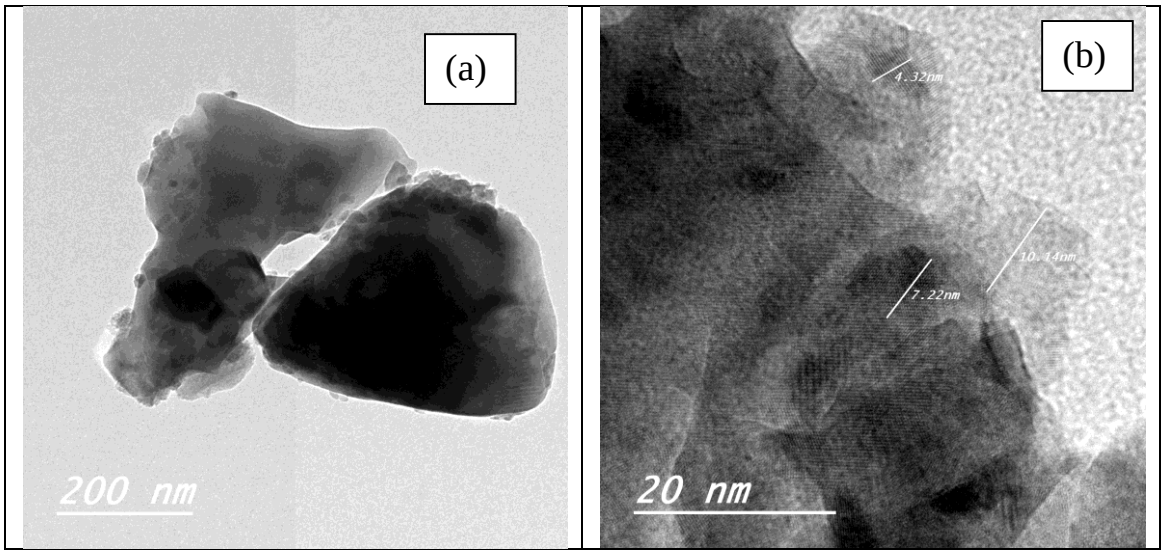


**Figure 2.** The TEM micrographs of the prepared n-TCP powder.

SEM micrograph of the prepared n-TCP powder is shown in Figure 3, displays a uniform and homogeneous network microstructure. The n-TCP powder is highly agglomerated with almost prismatic particles. The necking among the particles was apparent due to localized sintering at 800°C.

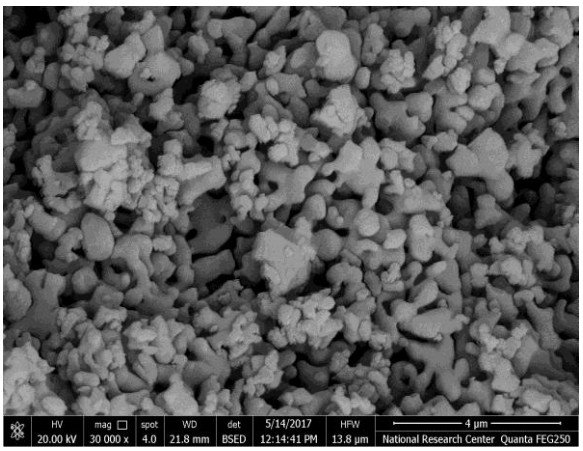


**Figure 3.** The SEM micrograph of the prepared n-TCP powder.

*3.2. Corrosion behavior of the uncoated Ti metal, Ti-6Al-4V, and Co-Cr-W alloys in artificial serum*

The change of the OCP with time for Ti metal, TAV, and Co-Cr-W alloys in the artificial serum is given in Figure 4. It is apparent from the results in this Figure that the OCP of Co-Cr-W alloy changes slightly to a more positive value throughout the first hour of immersion in serum and then a steady-state is reached. But for titanium and TAV alloy, the change in the OCP during the first hour of immersion in serum to a less negative value is observable and reaches a steady state. This shift of the OCP towards the more noble direction reveals the increase in the thickness of the air-formed passive film on the working materials in serum. The steady-state potential values follow the order Co-Cr-W > Ti > TAV. Previously it was found that the OCP of TAV in serum was shifted with time to more positive values gradually till about one hour and a steady-state was reached at the end [24]. In recent work, the OCP of Ti in sodium fluoride got more positive with time owing to the thickening of the passive oxide film on the metal [25].

The EIS was measured at the OCP value. Figure 5 presents the Nyquist impedance plots of the uncoated titanium metal, TAV, and Co-Cr-W alloys after immersion in serum for one hour. Figure 6 represents a two-time constants equivalent circuit for impedance data fitting. An electrical circuit similar to that used here was successfully applied for a two-layer structure film [26, 27]. The passive film on Ti [28] and TAV alloy [29, 30] consists of a barrier inner layer and a porous outer one and the identical advised circuit right here was used. The components of the circuit are $R_s$ electrolyte resistance, $C_p$ and $R_p$ capacitance, and resistance of the outer porous layer, and $C_b$ capacitance and $R_b$ resistance of the inner barrier one.

As a result of the deviation of the real capacitance from the pure one, a constant phase element (CPE) can be used for simulation of the impedance instead of the capacitance C. The CPE impedance is displayed using the following equation [31]: $Z_{CPE}=\frac{1}{S\,(j\,\omega)^n}$

where S is the frequency-independent real constant of the CPE and equals the idealized capacitance at $\omega = 1$, $\omega$ is the angular frequency ($\omega= 2\pi f$ rad $s^{-1}$), $j = \sqrt{-1}$, and n is the coefficient due to the deviation which varies between 1.0 for a perfectly smooth surface of pure capacitive behavior and 0.5 for a porous surface [32].

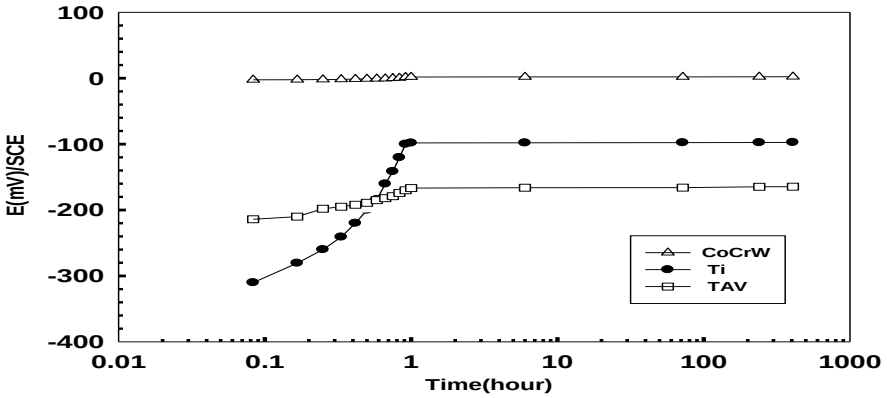


**Figure 4.** The change of the OCP with time for Ti metal, TAV, and Co-Cr-W alloys in serum.

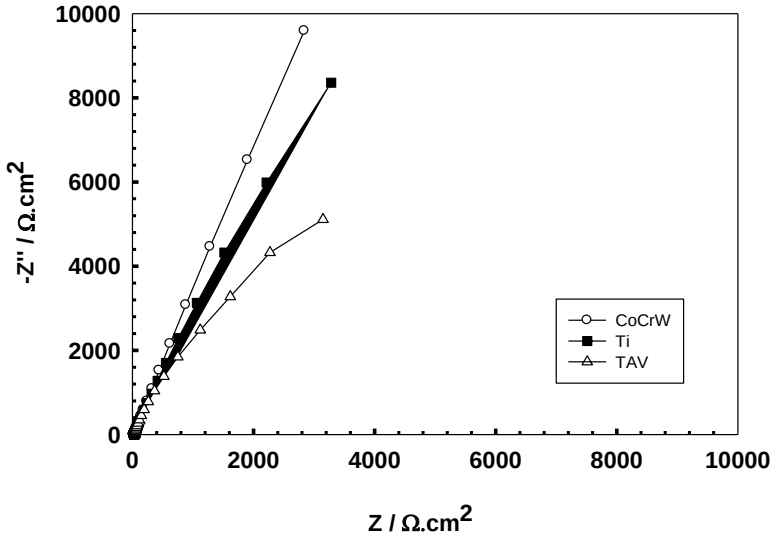


**Figure 5.** Nyquist plots of the uncoated titanium metal, TAV, and Co-Cr-W alloys after immersion in serum for one hour.

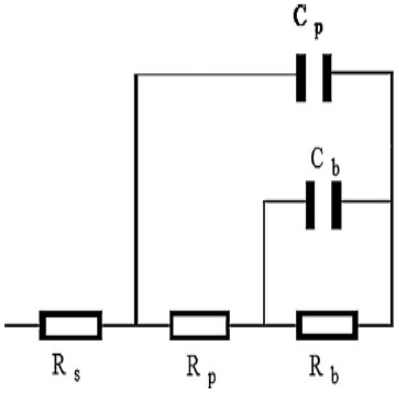


**Figure 6.** Equivalent circuit model for fitting the experimental results of impedance for titanium metal, TAV, and Co-Cr-W alloys

A similar circuit to that shown in Figure 6 was used before for fitting the impedance spectra of TAV alloy in serum [24]. This circuit gave wonderful fitting between the experimental results of the EIS and the theoretical ones. It is clear from Figure 5 that the impedance and consequently the corrosion resistance of the uncoated tested materials follows the order: TAV< titanium metal < Co-Cr-W, which is the same order of the steady-state OCP values of the same tested materials.

### *3.3. Corrosion behavior of n-TCP coated Ti metal, TAV, and Co-Cr-W alloys in artificial serum*

Coating of Ti metal, TAV, and Co-Cr-W alloys with n-TCP was described in the experimental section. The open-circuit potential of the n-TCP coated tested materials was followed with time for about 17 days in serum. As shown in Figure 7 the open circuit potentials of titanium and Co-Cr-W alloy increase positively in a short range of potential during the first hour of immersion in serum and reach steady-state values over the whole remaining time. For TAV alloy, an appreciable increase in the OCP to the more positive direction occurs for one hour before reaching the steady-state. The shifting of the OCP to a more noble value indicates the growth of the passive layer on the electrode surface under n-TCP coating. The process of passive layer thickening maybe occurs by diffusion of ions through the pores in the n-TCP coating layer. Also, the order of the steady-state potential values is the same as in the case of uncoated tested materials, i.e., Co-Cr-W > Ti > TAV.

Bode impedance plots of n-TCP coated titanium, TAV, and Co-Cr-W alloys after immersion in serum for different times, i.e. one hour, 7, and 21 days are shown in figure 8a-c. This Figure shows that for the three coated materials the impedance increases as the immersion time increases in serum from one hour to 7 days and then decreases after 21 days. This may be due to the partial breakdown of the passive film when reaches a certain thickness.

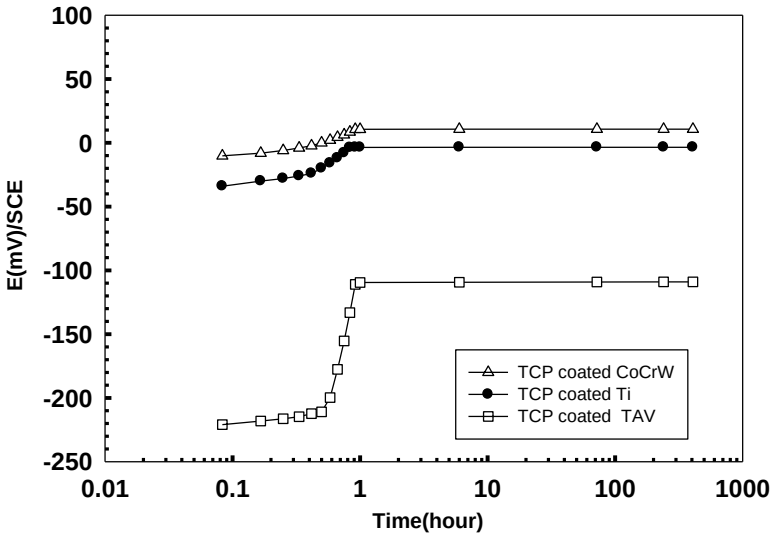


**Figure 7.** The change of the OCP with time for n-TCP coated titanium metal, TAV, and Co-Cr-W alloys in serum.

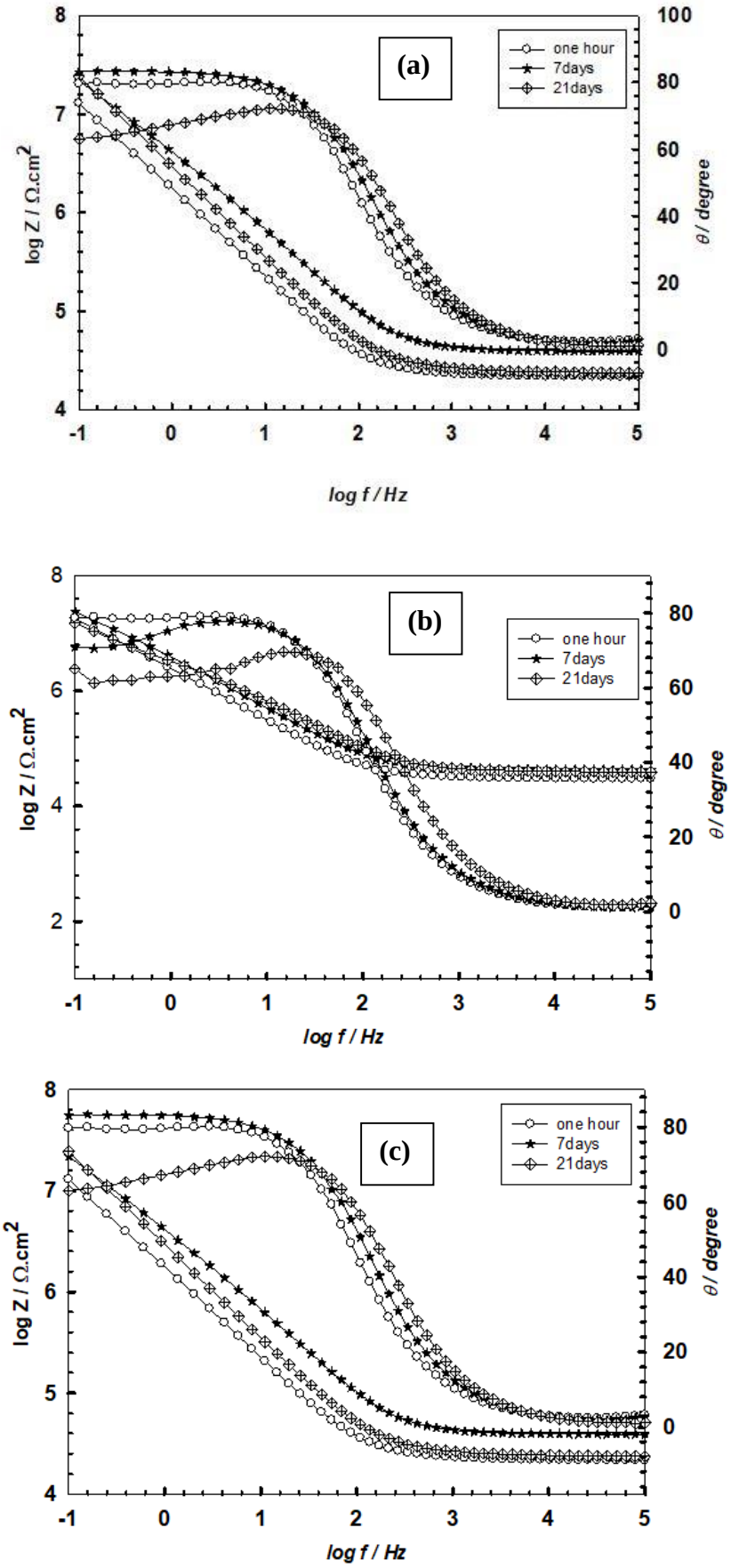


**Figure 8.** Bode plots of n-TCP coated (a) Co-Cr-W, (b) titanium and (c)TAV alloy after immersion in serum for different times.

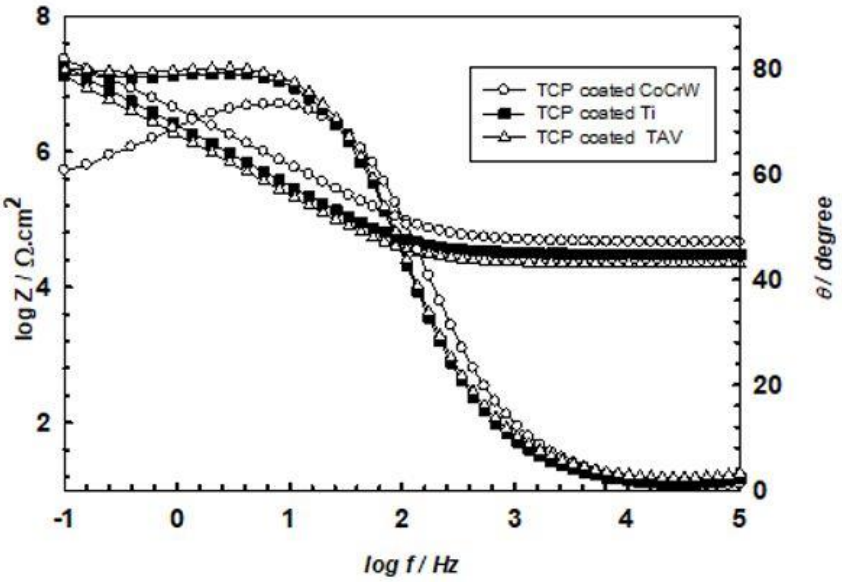


**Figure 9.** Bode plots for the n-TCP coated tested materials after one hour of immersion in serum.

The experimental results of the EIS of the n-TCP coated tested electrodes were fitted using the equivalent circuit in Figure 6. The fitted characteristic parameters for the three used materials are given in Table 3. From this Table, it is clear that the value of $R_b$ is larger than that of $R_p$.

**Table 3.** The parameters obtained from fitting the EIS data for uncoated and n-TCP coated Co-Cr-W, Ti, and TAV after immersion for different periods in serum.

| Material | Surface state | Time | $R_S$ ($\Omega.cm^2$) | Rp ($k\Omega.cm^2$) | $C_p$ ($\mu F.cm^{-2}$) | $R_b$ ($M\Omega.cm^2$) | $C_b$ ($\mu F.cm^{-2}$) |
|---|---|---|---|---|---|---|---|
| Co-Cr-W | Uncoated | One hour | 77.2 | 5.8 | 133.8 | 38.6 | 30 |
| | Coated with n-TCP | One hour | 83.1 | 7.2 | 125.6 | 46.9 | 14.8 |
| | | 7days | 85.1 | 8.6 | 115.5 | 55 | 11.3 |
| | | 21days | 80.5 | 6.3 | 130.8 | 44 | 19.9 |
| Ti element | Uncoated | One hour | 40 | 4.3 | 137.12 | 31.8 | 31.09 |
| | Coated with n-TCP | One hour | 51.8 | 6.7 | 128.78 | 45.1 | 15.2 |
| | | 7days | 59.2 | 8 | 118.7 | 53.2 | 12.5 |
| | | 21 days | 46.1 | 5.2 | 131.7 | 41 | 23.76 |
| Ti-6Al-4V | Uncoated | One hour | 31 | 3.4 | 138.09 | 29.8 | 33.1 |
| | Coated with n-TCP | One hour | 40.2 | 5.1 | 130.49 | 42.13 | 19.2 |
| | | 7days | 47.7 | 7.7 | 119.4 | 52.8 | 11.7 |
| | | 21days | 42.1 | 4.7 | 134.5 | 34.7 | 27.2 |

This means that the protection of the passive film formed on the tested materials is mainly due to the inner barrier layer which forms a large portion of the film. Also, from Table 3 we can see that for all the tested materials the values of $R_b$ and $R_p$ increase as the time of immersion increases from one hour to 7 days and after 21 days decrease again. The presence of two layers was indicated before for the passive film formed in the case of tetra calcium phosphate coated titanium in simulated body fluid and the film resistance increased with time to 3 h [5]. Previously the EIS plot of Ti electrode recorded at the OCP revealed that the deposition of calcium phosphate on the titanium surface caused an increase in polarization resistance in phosphate buffer solution [33]. At any immersion time the values of $R_b$ and $R_p$ are in the order Co-Cr-W > Ti > TAV similar to the order of the final values of the OCP. Bode plots for the n-TCP coated examined substances after one hour of immersion in serum are seemed in Figure 9 which verify the phenomena of corrosion resistance that follows the order Co-Cr-W > Ti > TAV.

### *3.4. Corrosion behavior of GO / CS /n-TCP composite coated Ti metal, TAV, and Co-Cr-W alloys in serum*

Coating of Ti metal, TAV, and Co-Cr-W alloys with GO / CS /n-TCP composite was described in detail in the experimental section. Figure 10 shows the change of the OCP with time in serum for the composite coated Ti metal, TAV, and Co-Cr-W alloys. As proven from this Figure the behavior of the OCP change remains the same as in the case of uncoated or n-TCP coated examined substances, i.e., the potential gets more positive in the first hour of immersion in serum and thereafter remains constant. Also, the order of increasing of the steady-state potentials does not change and remains as in the previous two cases of surface states, i.e., TAV < Ti < Co-Cr-W. The positive increase in the OCP gives further confirmation for the thickening of the protective layer on the electrode surface under the composite coating.

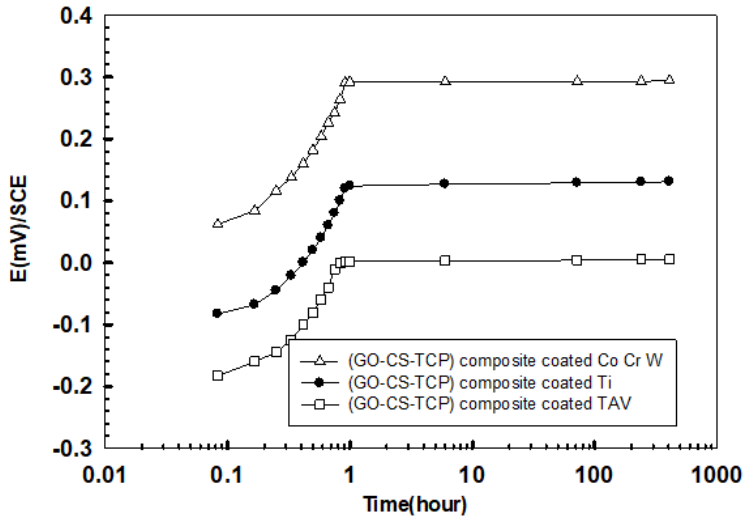


**Figure 10.** Change of the OCP with time in serum for GO/CS/n-TCP composite coated Ti metal, TAV, and Co-Cr-W alloys.

Bode impedance plots of the composite coated Ti metal, TAV, and Co-Cr-W alloys after immersion in serum for different time intervals 15, 60, and 180 min are shown in figure 11a-c. While bode plots after immersion times of 3, 7, and 21 days are presented in figure 12a-c. These figures show that for the three composite coated materials, the impedance increases with time in serum in the range from 15 min to 7 days and then decreases after 21 days due to the partial decomposition of the protective layer on the surfaces of the electrodes.

The fitting parameters obtained from the EIS data for the composite coated tested materials are presented in Table 4. In this Table, the values of $R_b$ and $R_p$ increase systematically with the increase of immersion time in serum up to 7 days and decrease again. The values of the two resistances follow the order Co-Cr-W > Ti > TAV.

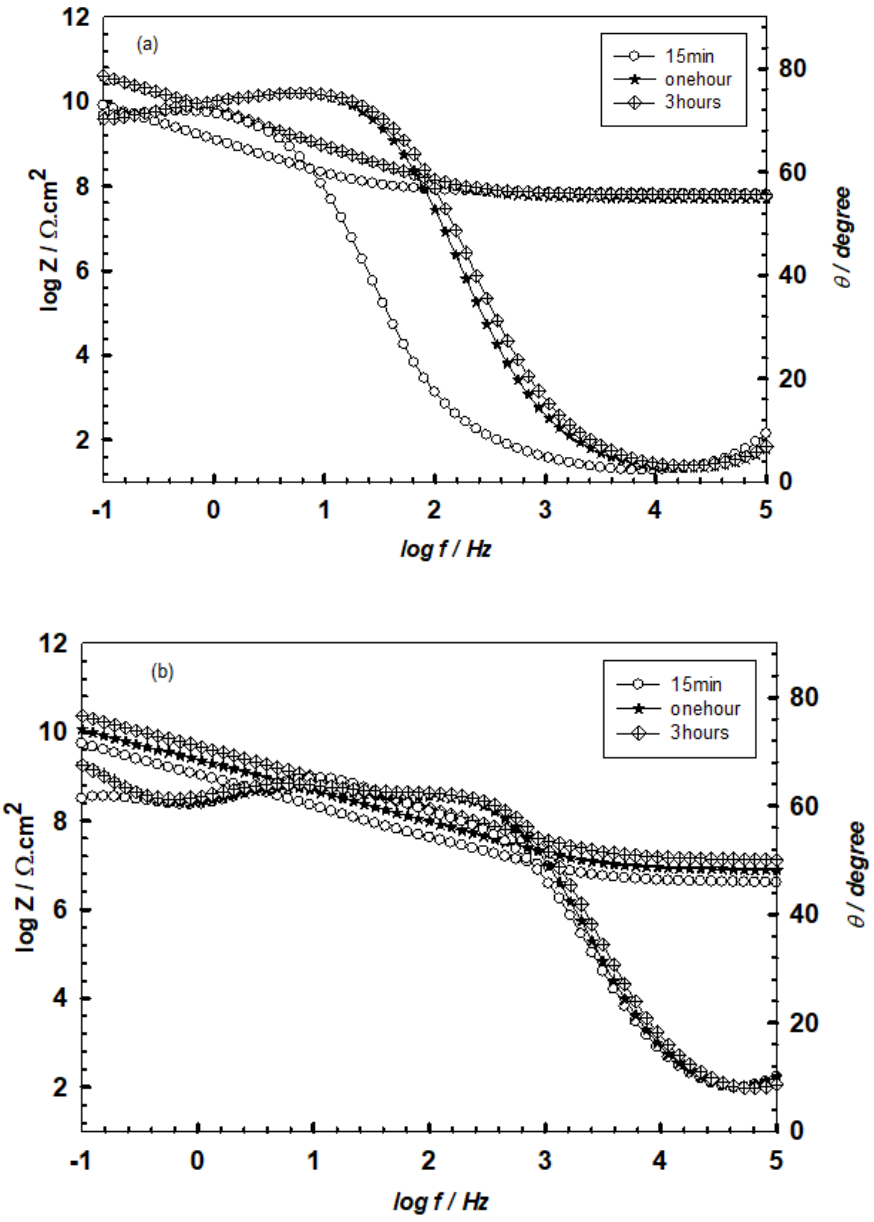

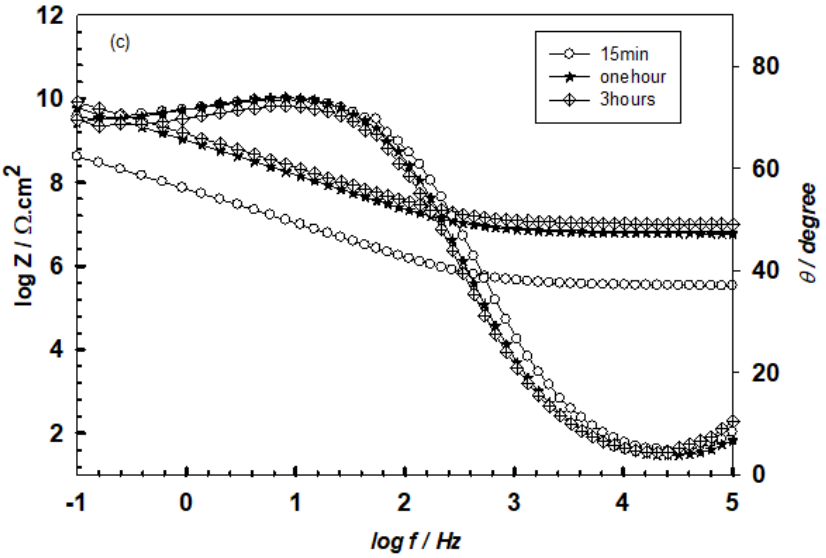


**Figure 11.** Bode plots of GO/CS/n-TCP composite coated (a) Co-Cr-W, (b)Ti metal, and(c)TAV after immersion in serum for different time intervals: 15, 60, and 180 min.

SEM is considered a good technique for identification the surface morphology of many metal matrix composites like that of titanium [34] and aluminum [35] and for pure bismuth metal [36]. SEM micrograph of the composite coated Co-Cr-W alloy is shown in Figure 13. It is clear from this photograph that the composite contains very small pores which help the diffusion of ions through the composite coating causing growth of the protective film with time on the metallic substance under investigation.

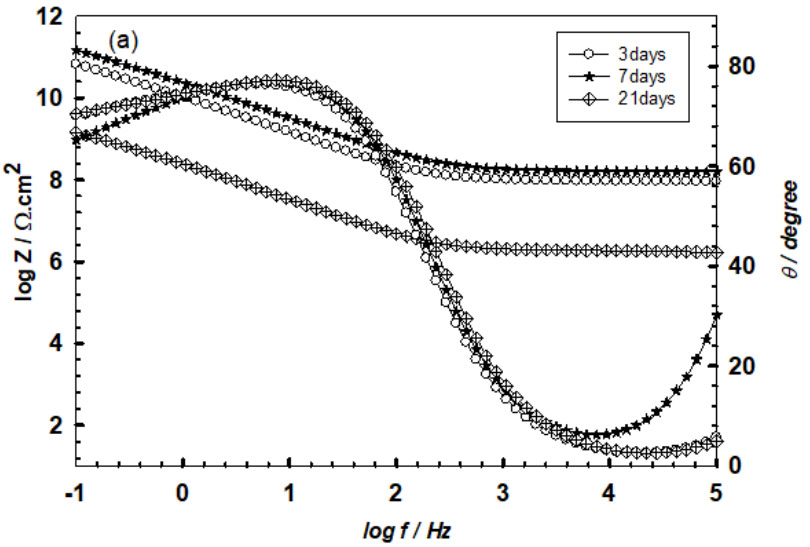

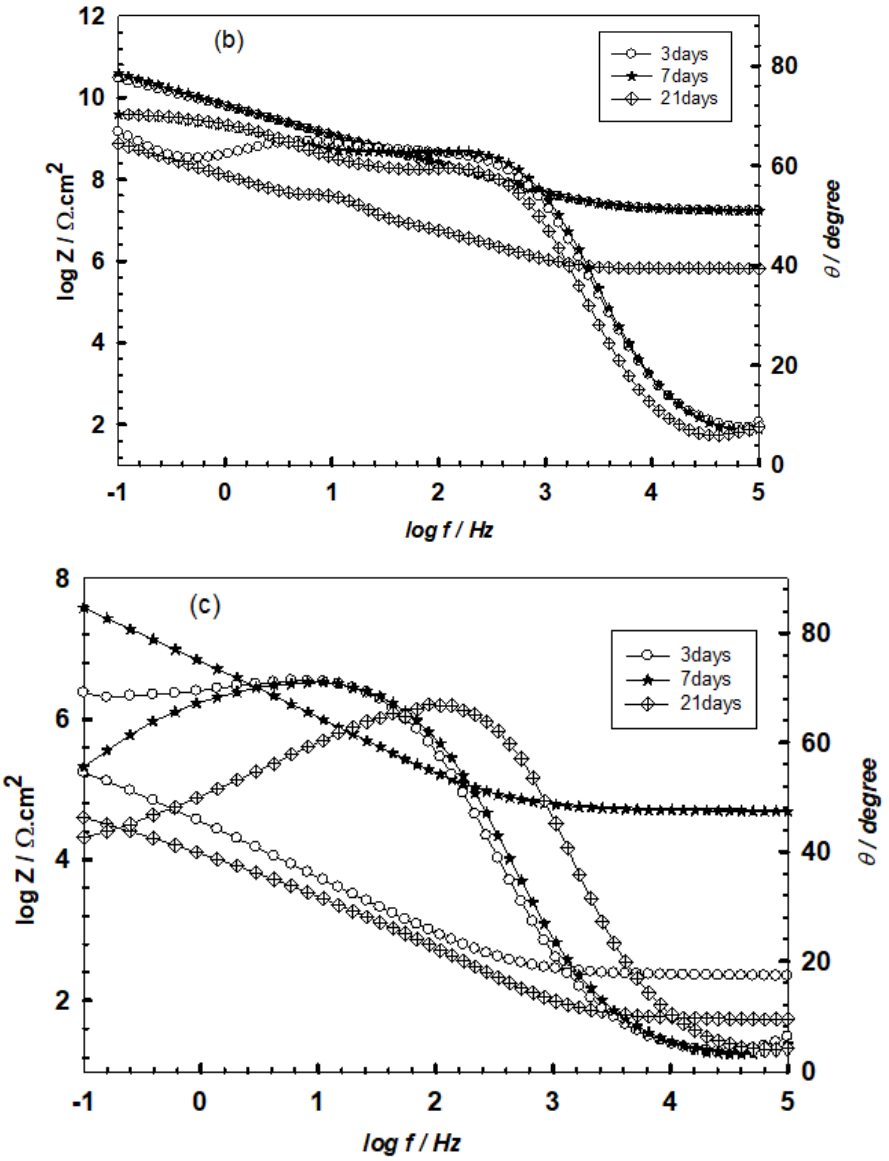


**Figure 12.** Bode plots of GO/CS/n-TCP composite coated (a) Co-Cr-W, (b)Ti metal, and(c)TAV after immersion in serum for different time intervals: 3, 7, 21 days.

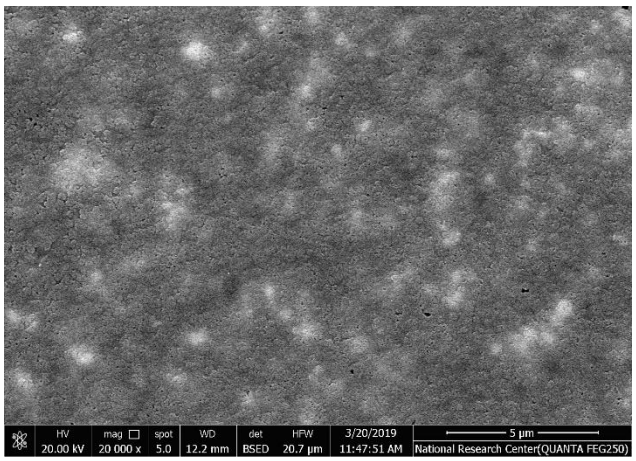


**Figure 13.** SEM photograph of GO/CS/n-TCP composite coated Co-Cr-W alloy.

**Table 4.** Electrochemical parameters were obtained from the EIS data for uncoated and GO/CS/n-TCP composite coated Co-Cr-W, Ti metal TAV after immersion in serum for different periods.

| Material | Surface state | Time | $R_S$ ($\Omega.cm^2$) | Rp ($k\Omega.cm^2$) | $C_p$ ($\mu F.cm^{-2}$) | $R_b$ ($M\Omega.cm^2$) | $C_b$ ($\mu F.cm^{-2}$) |
|---|---|---|---|---|---|---|---|
| Co-Cr-W | uncoated | One hour | 77.2 | 5.8 | 33.8 | 38.6 | 30 |
| | Coated with composite | 15min | 103 | 10.3 | 171 | 88 | 13.7 |
| | | One hour | 110 | 10.7 | 153 | 91 | 11.5 |
| | | 3hours | 114 | 11.2 | 130.6 | 93 | 10.8 |
| | | 3days | 121 | 11.8 | 129 | 96.7 | 9.6 |
| | | 7days | 134 | 12.6 | 127.5 | 99.1 | 8.7 |
| | | 21days | 138 | 11 | 142.1 | 92.2 | 11 |
| Ti element | uncoated | One hour | 40 | 4.3 | 37.12 | 31.8 | 31.09 |
| | Coated with composite | 15min | 89 | 9.1 | 191.2 | 77.1 | 17.1 |
| | | One hour | 91 | 9.7 | 185 | 79 | 15.7 |
| | | 3hours | 99 | 10.4 | 177.3 | 82.7 | 15.1 |
| | | 3days | 104 | 10.9 | 168.9 | 84.4 | 14 |
| | | 7days | 112 | 11.5 | 150.1 | 89.8 | 13.5 |
| | | 21 days | 114 | 10.1 | 171.9 | 79.8 | 15 |
| Ti-6Al-4V | uncoated | One hour | 31 | 3.4 | 38.09 | 29.8 | 33.1 |
| | Coated with composite | 15min | 77 | 7.8 | 210.1 | 50.29 | 20.1 |
| | | One hour | 79 | 8.2 | 195.4 | 53.12 | 19.2 |
| | | 3hours | 82 | 8.5 | 188.1 | 55,98 | 18.6 |
| | | 3days | 85 | 9 | 183 | 61.4 | 18.12 |
| | | 7days | 89.2 | 9.3 | 178 | 66.7 | 17.43 |
| | | 21days | 90 | 8 | 190 | 60.12 | 17.7 |

### *3.5. Comparison between the corrosion resistances of the three surface states of the tested materials in artificial serum*

From the change of the open circuit potential with time in serum for titanium metal, TAV, and Co-Cr-W alloys surfaces in the three states which are uncoated, coated with n-TCP, and coated with GO/CS/n-TCP composite (see Figures 4, 7, and 10) it is clear that the corrosion resistance of the three surface states for any one of the three tested materials increases according to the order: uncoated < n-TCP coated < GO/CS/n-TCP composite coated. Also, the impedance results in Table 4 show that for all the studied materials here the corrosion resistance of their surfaces follows the order uncoated < n-TCP coated < GO/CS/n-TCP composite coated. Therefore, EIS results conform to the open circuit potential measurements. Therefore, coating of the tested material surface with n-TCP or composite assists the process of the passive film growth with time till a definite thickness but for a long time, this protective layer dissolves to a certain limit.

## 4. CONCLUSION

The open-circuit potential of the uncoated, n-TCP coated and GO/CS/n-TCP composite coated titanium metal, TAV, and Co-Cr-W alloys in serum increases in the noble direction with increasing the immersion time, and this continued for about one hour before reaching a constant value revealing growth of the air-formed protective film on the surfaces of the materials. A two-time constants equivalent electrical circuit was suitable for the duplex in nature passive film on the examined materials. The EIS results indicated that the corrosion resistance increases with time and then decreases after 21 days due to the partial decomposition of the protective film on the electrode surfaces. The corrosion resistance of examined materials surfaces follows the order: uncoated <n-TCP coated< GO/CS/n-TCP composite coated. Coating of the tested materials surfaces with n-TCP or composite increases the process of the passive film growth with time till a definite thickness but for a long time, this protective layer dissolves to a certain limit. SEM micrograph of the composite coating on Co-Cr-W alloy revealed that the composite contains very small pores which help the diffusion of ions through the composite and leads to the growth of the passive film with time.

## References

1. F. Barrere, C.M. Van Der Valk, G. Meijer, R.A. Dalmeijer, K. De Groot and P. Layrolle, *J. Biomed. Mater Res. Part B*, 67 (2003) 655.
2. L.T. De Jonge, S.C.G. Leeuwenburgh, J.J.J.P. Van Den Beucken, J.T. Riet, W.F. Daamen, J.G.C. Wolke, D. Scharnweber and J.A. Janse, *Biomaterials*, 31 (2010) 2461.
3. S.C. Leeuwenburgh, J.G. Wolke, M.C. Siebers, J. Schoonman and J.A. Jansen, *Biomaterials*, 27 (2006) 3368.
4. O. Albayrak and S. Altintas, *J. Mater. Sci. Technol*., 26 (2010) 1006.
5. A. M. Fathi, H. K. Abd El-Hamid and M. M. Radwan, *Int. J. Electrochem. Sci.,* 11 (2016) 3164.
6. A.M.D. Campos, A. Sanchez, R. Gref, P. Calvo and M.J. Alonsoa, *Eur. J. Pharm. Sci*., 20 (2003) 73.
7. S.A. Agnihotri, N.N. Mallikarjuna and T.M. Aminabhavi*, J. Controlled Release*,100 (2004) 5.
8. A. Lahiji, A. Sohrabi and D. S. Hungerford, *J. Biomed. Mater. Res*., 51 (2000) 586.
9. S. Eissa, G.C. Jimenez and F. Mahvash, *Nano Res*., 8 (2014)1698.
10. J. Liu, L. Cui and D. Losic, *Acta Biomater*., 9 (2013) 9243.
11. R.Imani, S. H. Emami and S. Faghihi, *Phys. Chem. Chem. Phys*., 17 (2015) 6328.
12. F. Song, W.Hu and L. Xiao, *J. Biomater. Sci. Polym. Ed*., 26 (2015) 339.
13. J. F. Liao, Y. Qu and B. Y. Chu, *Sci. Rep*., 5 (2015)1.
14. S. Srivastava, V. Kumar and M.A. Ali, *Nanoscale*, 5 (2013) 3043.
15. Y. Wang, Z. Li and J. Wang, *Trends Biotechnol*., 29 (2011)205.
16. M. Nair, D. Nancy and A.G. Krishnan, *Nanotechnology*, 26 (2015)161001.
17. R. A. Ahmed, A.M. Fekry and R. A. Farghali, *Appl. Surf. Sci*., 285P (2013) 309.
18. Y. Y. Shi, M. Li, Q .Liu, Z. J. Jia, X. C. Xu, Y. Cheng and Y. F. Zheng, *J. Mater. Sci*., 27 (2016) 48.
19. B. Rikhari, S. P. Mani and N. Rajendran, *Carbohydr. Polym*., 189 (2018) 126.
20. A. Janković, S. Eraković, M. Mitrić, I. Z. Matić, Z. D. Juranić, G. C. P. Tsui, C. Tang, V. Mišković-Stanković, K.Y. Rhee and S.J.Park, *J. Alloys Compd*., 624 (2015) 148.
21. S.S. Khaloo, M.K. Amini, S. Tangestaninejad, S. Shahrokhian and R. Kia, *J. Iran. Chem. Soc.,* 1

(2004) 128.
22. S. P. Kunjalukkal, M. Chu, A. Balakrishnan, T. N. Kim and S. Cho, *Curr. Appl. phys*., 10 (2010) 68.
23. Reham H. Tammam, A. S. Mogoda and Mohamed H. Gharbawy, *Int. J. Electrochem. Sci*., 15 (2020) 8408.
24. A. M. Schmidt and D. S. Azambuja, *Mater. Res*., 6 (2003) 227.
25. A. S. Mogoda and K. M. Zohdy, *Int. J. Electrochem. Sci*., 15 (2020) 8070.
26. F. Mansfeld, *Electrochim. Acta*, 52 (2007) 7670.
27. B.Tian, D.B.Xie and F.H.Wang*, J.Appl. Electrochem*., 39 (2009) 447.
28. A. Robin and J. P. Meirelis, *J. Appl. Electrochem*., 37 (2007) 511.
29. Q. Qu, Y. He, L. Li, M. Yang, B. Lai and Y. Chen, *Int. J. Electrochem. Sci*., 10 (2015) 7453.
30. F. El-Taib Heakal, A. A. Ghoneim, A. S. Mogoda and Kh. A. Awad, *Corros. Sci*., 53 (2011) 2728.
31. K. Juttner, *Electrochim. Acta*, 35 (1990) 1501.
32. U. Rammelt and G. Reinhard, *Electrochim. Acta*, 35 (1990) 1045.
33. X. Cheng and S. G. Roscoe, *Biomaterials*, 26 (2005) 7350.
34. S Bose and T Nandi, *Bull. Mater. Sci*., 44 (2021) 46.
35. A.S. Mogoda, K.M. Zohdy and M.A. Aboutabl, *Silicon*, 12 (2021)1.
36. A.S. Mogoda, *Bull. Mater. Sci*., 43 (2020)1.